

Modeling and Identification of a Large Gap Magnetic Suspension System

David E. Cox * and Nelson J. Groom †

NASA Langley Research Center, Hampton, Virginia 23681-0001

Min-Hung Hsiao ‡, Jen-Kuang Huang §

Old Dominion University, Norfolk, VA 23529-0247

Abstract

This paper presents the results of modeling and system identification efforts on the NASA Large-Angle Magnetic Suspension Test Fixture (LAMSTF). The LAMSTF consists of a cylindrical permanent magnet which is levitated above a planar array of five electromagnets mounted in a circular configuration. The analytical model is first developed and open-loop characteristics are described. The system is shown to be highly unstable and requires feedback control in order to apply system identification. Limitations on modeling accuracy due to the effect of eddy-currents on the system are discussed. An algorithm is derived to identify a state-space model for the system from input/output data acquired during closed-loop operation. The algorithm is tested on both the baseline system and a perturbed system which has an increased presence of eddy currents. It is found that for the baseline system the analytic model adequately captures the dynamics, although the identified model improves the simulation accuracy. For the system perturbed by additional unmodeled eddy-currents the analytic model is no longer adequate and a higher-order model, determined through system identification, is required to accurately predict the system's time response.

* Research Engineer, Guidance and Controls Branch

† Senior Research Engineer, Guidance and Controls Branch

‡ Ph.D. student, Dept. of Mechanical Engineering

§ Associate Professor, Dept. of Mechanical Engineering

1 Introduction

The Large Angle Magnetic Suspension Test Fixture (LAMSTF) has been assembled by the NASA Langley Research Center for a ground-based experiment that will be used to investigate the technology issues associated with magnetic suspension at large gaps. This technology is applicable to future efforts that range from magnetic suspension of wind-tunnel models to advanced spacecraft isolation and pointing systems.

The LAMSTF system consists of a planar array of five electromagnets which actively suspend a small cylindrical permanent magnet (see Figure 1). The cylinder is a rigid body and has six independent degrees of freedom, namely, three displacements (x , y and z) and three rotations (pitch, yaw and roll). The roll axis of the cylinder is uncontrollable and is assumed to be motionless. A position sensing system is used to indirectly sense the pitch, yaw, x , y , and z position of the cylinder. It consists of six pairs of laser sheet sensors and photo-detectors mounted on a platform surrounding the suspended element. Therefore, the inputs consist of five currents into the electromagnets and the outputs are six voltage signals from the photo-detectors. The input currents to the electromagnets generate a magnetic field which produces a net force and torque on the suspended permanent magnet. Bias currents produce a force to counteract gravity. However, the field distribution about the suspension point produces forces which cause the suspension to be unstable. The linear model describes the systems dynamics in a region about this unstable equilibrium point. References [1] and [2] give a more complete description of the LAMSTF and some of the control approaches which have been investigated.

The analytical state-space model of LAMSTF is developed in Section 2. It has three highly unstable real poles and two low-frequency stable oscillatory modes. Experimental results obtained with controllers designed using the analytical model show reasonable agreement with simulation results. However, there are differences in predicted frequency and level of damping in the pitch axis. The differences are believed to be due to eddy-currents induced in the electromagnet's iron cores which are not considered in the system model. The objective of this paper is to derive the analytical model for a large-gap magnetic suspension system, and to demonstrate system identification as a method of eliminating model errors due to eddy-currents.

In the past few decades, a great variety of system identification methods have been studied. The choice of an identification method depends on the nature of the system and the purpose of identification. For control of a dynamic system, the state-space model is usually preferred. Recently, some methods were introduced [3] - [5] to identify a state-space model from a finite difference model. The difference model, called Auto-Regressive with eXogenous input (ARX) model, is derived through Kalman filter theories. This derivation is based on a deterministic approach. For identifying linear stochastic systems, projection filters are required as developed in [6] and [7]. There, the relationship between the state-space model and the ARX model was derived based on optimal estimation theory. In Section 4 this relationship is re-derived in a much simpler way through a z -transform of the ARX model.

Since the LAMSTF system is highly unstable, feedback control is required to ensure overall system stability while obtaining input/output data. The identification algorithm is applied to identify a state-space model from the plant input to the plant output. This system identification includes the following steps. First, the coefficient matrices of an ARX model, which can represent the corresponding state-space model, are estimated from the plant input/output data via the least-squares method. Second, the system and Kalman filter Markov parameters are computed from the estimated coefficient matrices of the ARX model in a recursive way. Third, the system matrices are realized from Hankel matrices formed by the system Markov parameters via the singular-value decomposition method [8], [9].

Experimental results are presented in Section 5. Step responses from simulations and test data are used to compare the accuracy of identified models of the baseline and perturbed system with the analytic model. It is found that the analytical model has a deficiency which is most evident in the dynamics of the pitch axis. Previous work with this system [2], [10] showed that increasing eddy-currents by placing an aluminum ring around the suspended element increases the modeling error in the pitch dynamics. For the baseline system the analytic model adequately captures the dynamics, although the identified model improves the simulation accuracy. For the system perturbed by an aluminum ring the unmodeled eddy-currents produce larger errors in pitch response and a higher-order model, determined through system identification, is required to accurately predict the system's time response.

2 System Modeling

A representation of this system is shown in Figure 1. The motion of the cylinder is defined by the body fixed axes, $\bar{x}, \bar{y}, \bar{z}$, that define the motion of the cylinder with respect to fixed inertial axes x, y, z . The development here follows the approach detailed in [11] and [12].

In a large-gap magnetic suspension system torques on the suspended element in the inertial coordinate system can be approximated as,

$$T_c = \int_V (M \times \mathcal{B}) dV \approx \nu (M_o \times \mathcal{B}_o) \quad (1)$$

and forces as,

$$F_c = \int_V (M \cdot \nabla) \mathcal{B} dV \approx \nu (M_o \cdot \nabla) \mathcal{B}_o = \nu [\partial \mathcal{B}_o] M_o \quad (2)$$

where ν is the volume of the permanent magnet core, M is the magnetization of the core, \mathcal{B} is the flux density, and $\partial \mathcal{B}$ is a matrix of gradients. The approximation assumes that the magnetization is uniform over the core volume and that the higher order terms, obtained by expanding \mathcal{B} about the origin of the core axis system are negligible.

In body fixed coordinates, the torque becomes

$$\bar{T}_c \approx \nu (\bar{M}_o \times T_m \mathcal{B}_o) \quad (3)$$

and the corresponding force,

$$\bar{F}_c \approx \nu T_m [\partial \mathcal{B}_o] T_m^{-1} \bar{M}_o \quad (4)$$

where T_m is an Euler transformation matrix between the inertial and body fixed coordinate systems. Under small angle and rate assumptions we can write the angular and linear acceleration of the suspended element, $\dot{\bar{\Omega}}, \dot{\bar{V}}$ in the body fixed coordinates as

$$\dot{\bar{\Omega}} = I_c^{-1} (\bar{T}_c + \bar{T}_d) \quad (5)$$

$$\dot{\bar{V}} = m_c^{-1} (\bar{F}_c + \bar{F}_d) \quad (6)$$

where I_c, m_c is the inertia and mass, respectively, of the suspended element; \bar{T}_c and \bar{F}_c denote the control torques and forces produced by the electromagnets; and \bar{T}_d and \bar{F}_d denote external disturbance torques and forces. For LAMSTF the only significant disturbance acting on the suspended element is along the z-axis and is equal to its weight

$$\bar{F}_g = T_m \begin{bmatrix} 0 & 0 & -m_c g \end{bmatrix} \quad (7)$$

where g is the acceleration due to gravity.

The control torques and forces are functions of position and orientation as well as the input currents, thus the equations of motion are in the form

$$\dot{x} = f(\tilde{x}, I) = \left\{ \begin{array}{l} I_c^{-1} \bar{T}_c(\tilde{x}, I) \\ m_c^{-1} (\bar{F}_c(\tilde{x}, I) + \bar{F}_d) \end{array} \right\} \quad (8)$$

where,

$$x = \left[\tilde{x} \quad \Omega_{\bar{y}} \quad \Omega_{\bar{z}} \quad V_{\bar{x}} \quad V_{\bar{y}} \quad V_{\bar{z}} \right]^T, \quad (9)$$

and \tilde{x} is the position and orientation of the body fixed reference frame with respect to the inertial frame. The equation can be linearized around the nominal operation point (x_o, I_o) by performing a Taylor series expansion. Neglecting second-order terms and subtracting out x_o results in

$$\delta \dot{x} = A \delta x + B \delta I, \quad (10)$$

where $A = \frac{\partial f}{\partial x} \Big|_{x_o, I_o}$ and $B = \frac{\partial f}{\partial I} \Big|_{x_o, I_o}$. The eigenvalues and mode shapes of the analytic model for LAMSTF are shown in Table 1 and Figure 2, respectively.

The development above yields a linear system model which is valid under the stated assumptions. In practice these assumptions are not overly constraining and are met by the LAMSTF system. The planar arrangement of electromagnets leads to a symmetric field distribution, and the suspended element is a uniform cylindrical magnet. Another factor, however, which is not considered in the model is the dynamic effects of nearby conductors on the magnetic fields. The actuator coils in LAMSTF contain iron cores which greatly improve their efficiency. The field in the cores is kept below the saturation level for that material so hysteresis effects are minimal. However, eddy currents due to changing magnetic fields can add dynamics to the actuator. Currently the system is modeled using a numerical package

Analytic Model	Nominal Identified	Perturbed Identified
0.00 - 0.96i	1.04 - 12.09i	0.54 - 10.22i
0.00 + 0.96i	1.04 + 12.09i	0.54 + 10.22i
0.00 - 7.97i	0.75 - 7.38i	2.02 - 9.22i
0.00 + 7.97i	0.75 + 7.38i	2.02 + 9.22i
-9.78	-6.71	-6.16
9.78	6.53	7.16
-57.81	-56.95	-57.95
57.81	61.72	60.33
-58.78	-58.14	-58.48
58.78	62.76	62.65
		-256.2

Table 1: Continuous plant eigenvalues for analytic model and identified models, under nominal and perturbed conditions.

which considers the static effect iron cores have on the field distribution of each actuator. The software cannot, however, predict the dynamic effect of eddy-currents in the iron cores.

In general eddy current effects are difficult to model because the relevant material properties vary with frequency and the resulting field distortion depends upon the conductor's geometry. Within a conductor the effect of eddy-currents is purely dissipative. Fields arise from eddy-currents which exactly oppose the inducing fields and are proportional to the inducing fields time rate-of-change. However, at points outside the conductor, fields may add in-phase with the suspension fields. For applications where magnetic suspension systems must operate in the vicinity of complex conductors, detailed modeling of eddy-currents is difficult if not impossible. For this reason it is desirable to investigate the use of system identification to refine the analytic models of these systems.

3 Relation Between State-Space and ARX Models

A finite-dimensional, linear, discrete-time, time-invariant system can be modeled as:

$$x_{k+1} = Ax_k + Bu_k + w_k, \quad (11)$$

$$y_k = Cx_k + Du_k + \nu_k, \quad (12)$$

where $x \in R^{n \times 1}$, $u \in R^{s \times 1}$, $y \in R^{m \times 1}$ are state, input and output vectors, respectively; w_k is the process noise, ν_k the measurement noise; $[A, B, C, D]$ are the state-space parameters. Sequences w_k and ν_k are assumed Gaussian, white, zero-mean, and stationary with covariance matrices Q and R , respectively. One can derive a steady-state filter innovation model [6]

$$\hat{x}_{k+1} = A\hat{x}_k + Bu_k + AK\epsilon_k, \quad (13)$$

$$y_k = C\hat{x}_k + Du_k + \epsilon_k \quad (14)$$

where \hat{x}_k is the a priori estimated state, K is the steady-state Kalman filter gain and ϵ_k is the residual after filtering: $\epsilon_k = y_k - C\hat{x}_k - Du_k$. The existence of K is guaranteed if the system is detectable and $(A, Q^{1/2})$ is stabilizable. Substituting (14) into (13), one has

$$\hat{x}_{k+1} = \bar{A}\hat{x}_k + \bar{B}u_k + AKy_k, \quad (15)$$

where $\bar{A} = A - AKC$, $\bar{B} = B - AKD$, and \bar{A} is guaranteed to be asymptotically stable because the steady-state Kalman filter gain K exists. Taking the z-transform of (15) and (14), one has

$$\hat{x}(z) = (z - \bar{A})^{-1}(\bar{B}u(z) + AKy(z)), \quad (16)$$

$$y(z) = C\hat{x}(z) + Du(z) + \epsilon(z). \quad (17)$$

Substituting (16) into (17) yields,

$$y(z) = C(z - \bar{A})^{-1}(\bar{B}u(z) + AKy(z)) + Du(z) + \epsilon(z) \quad (18)$$

Taking the inverse z-transform of (18) with $(z - \bar{A})^{-1} = \sum_{i=1}^{\infty} \bar{A}^{i-1}z^{-i}$, one has

$$y_k = \sum_{i=1}^{\infty} C\bar{A}^{i-1}AKy_{k-i} + \sum_{i=1}^{\infty} C\bar{A}^{i-1}\bar{B}u_{k-i} + Du_k + \epsilon_k \quad (19)$$

Since \bar{A} is asymptotically stable, $\bar{A}^i \approx 0$ if $i > q$ and q is chosen large enough. Thus (19) becomes

$$y_k \approx \sum_{i=1}^q a_i y_{k-i} + \sum_{i=0}^q b_i u_{k-i} + \epsilon_k, \quad (20)$$

where, $a_i = C\bar{A}^{i-1}AK$, $b_i = C\bar{A}^{i-1}\bar{B}$, and $b_0 = D$.

The model described by (20) is called the Auto-Regressive with eXogenous input (ARX) model which directly represents the relationship between output and input without state variables. The coefficient matrices a_i and b_i can be estimated through least-squares methods from random excitation input u_k and the corresponding output y_k . From (20) and for l points of the input/output data, one can have

$$\xi \approx \theta\Phi + \Xi \quad (21)$$

where,

$$\begin{aligned} \xi &= \begin{bmatrix} y_{q+1} & y_{q+2} & \cdots & y_l \end{bmatrix}, \\ \theta &= \begin{bmatrix} b_0 & a_1 & b_1 & a_2 & b_2 & \cdots & a_q & b_q \end{bmatrix}, \\ \Xi &= \begin{bmatrix} \epsilon_{q+1} & \epsilon_{q+2} & \cdots & \epsilon_l \end{bmatrix}, \\ \Phi &= \begin{bmatrix} u_{q+1} & u_{q+2} & \cdots & u_l \\ \phi_q & \phi_{q+1} & \cdots & \phi_{l-1} \\ \phi_{q-1} & \phi_q & \cdots & \phi_{l-2} \\ \vdots & \vdots & \ddots & \vdots \\ \phi_1 & \phi_2 & \cdots & \phi_{l-q} \end{bmatrix}, \text{ and } \phi = \begin{bmatrix} y \\ u \end{bmatrix} \end{aligned}$$

From (21) it can be seen that parameters of the ARX model are linearly related to the input/output data. Therefore, solving for an ARX model involves solving a linear system involving an over determined set of equations. The batch least-square solution for the coefficient matrices a_i and b_i is

$$\theta = \xi \Phi^\dagger \quad (22)$$

where Φ^\dagger is the pseudoinverse of the Φ matrix.

4 Markov Parameters and State-Space Realization

The previous section presents the relation between an ARX model and a state-space model. The ARX model can be estimated through the least-squares method. The estimated ARX model has to be transformed back to a state-space model for system model comparisons or controller designs. First, the system and Kalman filter Markov parameters are calculated from the estimated coefficient matrices of the ARX model. Then a state-space realization can be obtained by using singular-value decomposition for a Hankel matrix formed by the system Markov parameters.

4.1 System and Kalman Filter Markov Parameters

Taking the z-transform of state-space model (13), one has

$$\hat{x}(z) = (z - A)^{-1}(Bu(z) + AK\epsilon(z)). \quad (23)$$

Substituting (23) into the z-transform of the output equation (14) yields

$$y(z) = C(z - A)^{-1}(Bu(z) + AK\epsilon(z)) + Du(z) + \epsilon(z) \quad (24)$$

$$= \sum_{k=0}^{\infty} Y(k)z^{-k}u(z) + \sum_{k=0}^{\infty} N(k)z^{-k}\epsilon(z) \quad (25)$$

where $Y(0) = D$ and $Y(k) = CA^{k-1}B$ are called system Markov parameters, $N(0) = \tilde{I}$ an identity matrix, and $N(k) = CA^kK$ the Kalman filter Markov parameters.

Taking the z-transform of the ARX model (20), one has

$$\left(\tilde{I} - \sum_{i=1}^q a_i z^{-i} \right) y(z) = \sum_{i=0}^q b_i z^{-i} u(z) + \epsilon(z) \quad (26)$$

Applying long division to (26), one has

$$\begin{aligned} y(z) &= (b_0 + (b_1 + a_1 b_0)z^{-1} \\ &+ (b_2 + a_1(b_1 + a_1 b_0) + a_2 b_0)z^{-2} + \dots)u(z) \\ &+ (\tilde{I}a_1 z^{-1} + (a_1 a_1 + a_2)z^{-2} + (a_1(a_1 a_1 + a_2) + a_2 a_1 + a_3)z^{-3} + \dots)\epsilon(z) \end{aligned} \quad (27)$$

By comparing with (25), the system and Kalman filter Markov parameters can be recursively calculated from the estimated coefficient matrices of the ARX model as follows

$$Y(k) = b_k + \sum_{i=1}^k a_i Y(k-i) \quad (28)$$

$$N(k) = \sum_{i=1}^k a_i N(k-i) \quad (29)$$

It is noted that $Y(0) = b_0$, $N(0) = \tilde{I}$, and $a_i = b_i = 0$, when $i > q$. One may obtain (28) and (29) from (20) and the definition of the Markov parameter [4],[5]. However, the derivation is much more complex. The Markov parameters of the Kalman filter can be used to design an optimal estimator without requiring noise statistics. The system Markov parameters are used in the following section to form the state-space model.

4.2 State-Space Realization

To obtain the open-loop state-space model, the realization through Singular Value Decomposition (SVD) method [8], [9] is used. The first step is to form a Hankel matrix from the system Markov parameters as follows:

$$H(j) = \begin{bmatrix} Y(j) & Y(j+1) & \cdots & Y(j+\beta) \\ Y(j+1) & Y(j+2) & \cdots & Y(j+\beta+1) \\ \vdots & \vdots & \ddots & \vdots \\ Y(j+\gamma) & Y(j+\gamma+1) & \cdots & Y(j+\gamma+\beta) \end{bmatrix} \quad (30)$$

where $Y(j)$ is the j -th Markov parameter. From the measurement Hankel matrix, The realization uses the SVD of $H(1)$, $H(1) = U\Sigma V^T$, to identify an n -th order discrete state-space model as

$$A = \Sigma_n^{-1/2} U_n^T H(2) V_n \Sigma_n^{-1/2}, B = \Sigma_n^{1/2} V_n^T E_s, C = E_m^T U_n \Sigma_n^{1/2}, D = Y(0) \quad (31)$$

where matrix Σ_n is the upper left hand $n \times n$ partition of Σ containing the n largest singular values along the diagonal. Matrices U_n and V_n are obtained from U and V by retaining only the n columns of singular vectors associated with the n singular values. Matrix E_m is a matrix of appropriate dimension having m columns, all zero except that the top $m \times m$ partition is an identity matrix. E_s is defined analogously.

5 Numerical and Experimental Results

A number of experimental tests were conducted to both validate the analytic modeling procedure and to demonstrate system identification as a method of generating models which

include eddy current effects. A control law was designed, based on the analytic model, to achieve approximate pole-placement [13]. The continuous control design was then converted to a discrete system via a tustin approximation. Real-time code implemented the controller at 250 Hz and provided reference inputs and data storage. A system simulation was also developed. The simulation was based on the discrete controller and used both the analytic and identified models for comparison.

To validate the analytic model a series of step responses were taken and compared to simulation. Inputs were placed at the system's sensors to achieve a unity feedback tracking system, as shown in Figure 3. The tracking signal was a series of steps in θ_y, θ_z, x, y and z with magnitudes of 2 degrees angular and 1 mm linear. Although the system does not track the reference perfectly, for most degrees of freedom simulation results match the experimental results as shown in figure 4. The analytical model lacks some cross-coupling in yaw, and has a different damping and frequency in pitch dynamics. A step response in pitch is shown in Figure 5 along with its simulation.

System identification tests were run to try and improve the model accuracy. A white noise reference input was placed at the control coils as shown in Figure 3. Data was recorded from the plant input and plant output. The recorded data length was 6000 points for each of the five actuators and six sensors. The model order was chosen to be 15, large enough to capture the dynamics of the system. From the Markov parameters a 10th order state-space model was derived. Using this identified model the tracking response was simulated. The simulated response compared well with the experimental response even in pitch, which is shown in Figure 6.

In order to study the effects of eddy-currents a conductive structure was added to perturb the nominal system. The perturbed system included an aluminum ring around the suspended element, as shown in Figure 7. The aluminum ring produces eddy-currents in response to changes in the magnetic fields but does not cause a static warping of the fields. This adds dynamics which are not considered in the analytic model. Previous experiments (which used an aluminum ring to mount the sensor array) had shown this geometry to cause modeling errors primarily in dynamics of the pitch axis. Using the same controller as before, step responses were taken for the perturbed configuration. The experimental pitch response of both the nominal and perturbed systems are shown in Figure 8. As evidenced from the figure, the effect of the aluminum ring is dramatic, causing a significant loss of damping in the closed-loop response.

System identification tests were repeated on the perturbed system. As before, white noise was injected at the systems actuators and a total of 6000 data points were taken at the input and output of the plant. The resulting system model included the effects of eddy-currents and was able to accurately predict the response in pitch as well as in other degrees of freedom. The pitch response of the experimental perturbed system and the simulation with the identified model are shown in Figure 9.

The eigenvalues of the analytic model, the identified model of the nominal system, and the identified model of the perturbed system are compared in Table 1. Two points are to be

noted here. First is that the perturbed model has an additional real pole. It was not possible to obtain a 10th order model which would accurately match the system's time response. An 11th order model, however, with an additional real pole, did match the experiment quite well. Although the pole is much higher in frequency than the nominal model dynamics, it is important for the closed-loop dynamics and adds the type of phase errors expected from eddy-current effects.

The second point is that the neither identified model contains the low frequency stable eigenvalues corresponding to the analytic model. This is believed to be an error in the identified model which has a negligible effect on the closed-loop performance. In obtaining bounded input/output data for identification, feedback control is required to provide overall system stability. Under closed-loop operation, however, it is difficult to guarantee sufficiently rich input to the plant to excite all the systems dynamics. In practice it was found that the low frequency oscillatory modes associated with the motion in the z -axis were difficult to identify. It is believed that, due to the controllers large low frequency gain, the white noise input, which acts as a disturbance, did not induce sufficient low frequency power at the plant input.

6 Concluding Remarks

An analytical model is derived for an unstable large-gap magnetic suspension system. This model is linearized to provide an analytic state-space model. The linear model dynamics are described and validated through experimental testing. A method of system identification is also described. The relation between the state-space and ARX models is derived through z -transforms. This derivation provides physical interpretation of the mapping from input/output data to the state space and the explicit meanings of the ARX parameters. Applying the system identification algorithms to the experimental system yields models with improved fidelity. Experimental tests are also conducted to show the effect of unmodeled eddy-currents on the closed-loop system. Applying system identification yields models for the perturbed system which include eddy-currents. These models are also validated through comparison of closed-loop step responses.

References

- [1] N. J. Groom, and C. P. Britcher: *A Description of a Laboratory Model Magnetic Suspension Test Fixture with Large Angular Capability*. Proceedings of the First IEEE Conference on Control Application, Sept. 13-16, 1992 Dayton, OH, Vol. 1, pp. 454-459.
- [2] C. P. Britcher and L. E. Foster: *Some Further Developments in the Dynamic Modeling and Control of the Large Angle Magnetic Suspension Test Fixture*. Proceedings of the Second International Symposium on Magnetic Suspension Technology, Seattle WA, August 1993, pp. 367-377.
- [3] C. W. Chen, J.-K. Huang, M. Phan, and J.-N. Juang: *Integrated System Identification and Modal State Estimation for Control of Flexible Space Structures*. Journal of Guidance, Control and Dynamics, 1992, Vol 15, No.1, 88-95.
- [4] M. Phan, L. G. Horta, J.-N. Juang, and R. W. Longman: *Linear System Identification via an Asymptotically Stable Observer*. AIAA Guidance, Navigation and Control Conference, 1991.
- [5] J. N. Juang, M. Phan, L. G. Horta, and R. W. Longman: *Identification of Observer/Kalman Filter Markov Parameters: Theory and Experiments*. AIAA Guidance, Navigation and Control Conference 1991, and NASA TM-104069.
- [6] C. W. Chen, J.-K. Huang, and J.-N. Juang: *Identification of Linear Stochastic Systems Through Projection Filters*. AIAA Structures, Structural Dynamics and Materials Conference 1992, pp. 2330-2340. Also to appear in Journal of Guidance, Control and Dynamics.
- [7] C. W. Chen, J.-N. Juang, and J.-K. Huang: *Adaptive Linear System Identification and State Estimation*. Control and Dynamic Systems: Advances in Theory and Applications, Vol. 57, Multidisciplinary Engineering Systems: Design and Optimization Techniques and Their Application, edited by C. T. Leondes. New York: Academic Press, Inc., 1993, pp. 331-368.
- [8] C. T. Chen, 1984, *Linear System Theory and Design*, Second Edition, Chapter 6, CBS College Publishing, New York.
- [9] J. N. Juang, and R. S. Pappa: *An Eigensystem Realization Algorithm for Modal Parameter Identification and Model Reduction*. Journal of Guidance, Control, and Dynamics, 1985, Vol. 8, No. 5, 620-627.
- [10] K. B. Lim, and D. E. Cox: *Experimental Robust Control Studies on an Unstable Magnetic Suspension System*. Proceedings of the American Control Conference, Baltimore, MD, July 1994, pp. 3198-3203.
- [11] N. J. Groom: *Analytical Model of a Five Degree-Of-Freedom Magnetic Suspension and Positioning System*. NASA TM-100671, 1989.

- [12] N. J. Groom, and C. P. Britcher: *Open-Loop Characteristics of Magnetic Suspension Systems Using Electromagnets Mounted in a Planar Array*. NASA TP-3229, 1992.
- [13] N. J. Groom: *A Decoupled Control Approach for Magnetic Suspension Systems Using Electromagnets Mounted in a Planar Array*. NASA TM-109011, 1993.

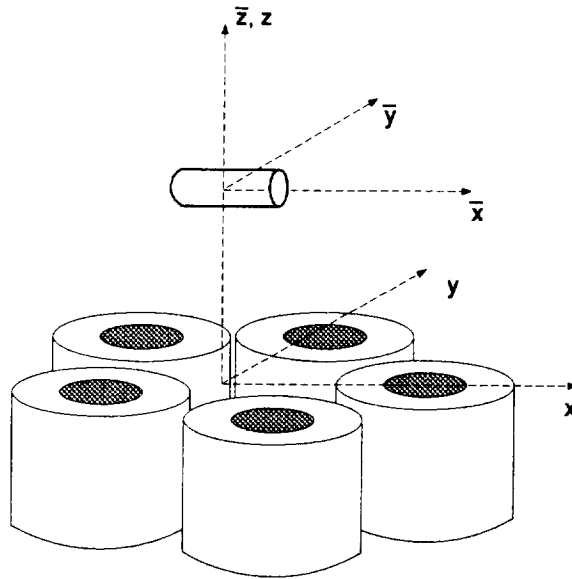


Figure 1: LAMSTF Physical system

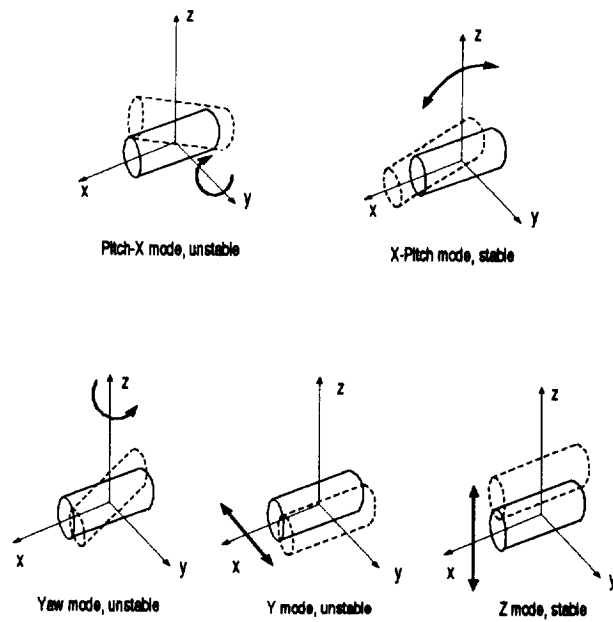


Figure 2: LAMSTF Modeshapes

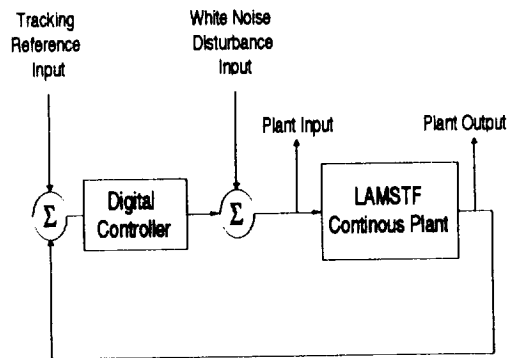


Figure 3: Block diagram for experimental LAMSTF system

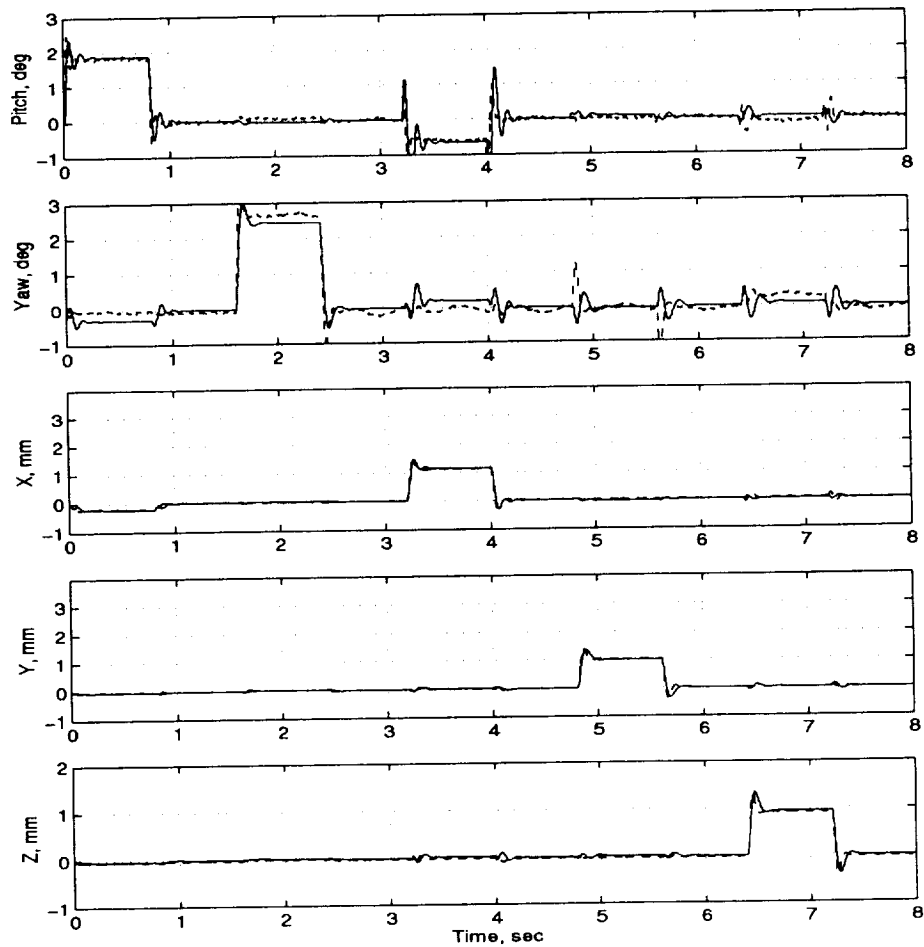


Figure 4: Analytic model simulation (solid) and experiment (dashed)

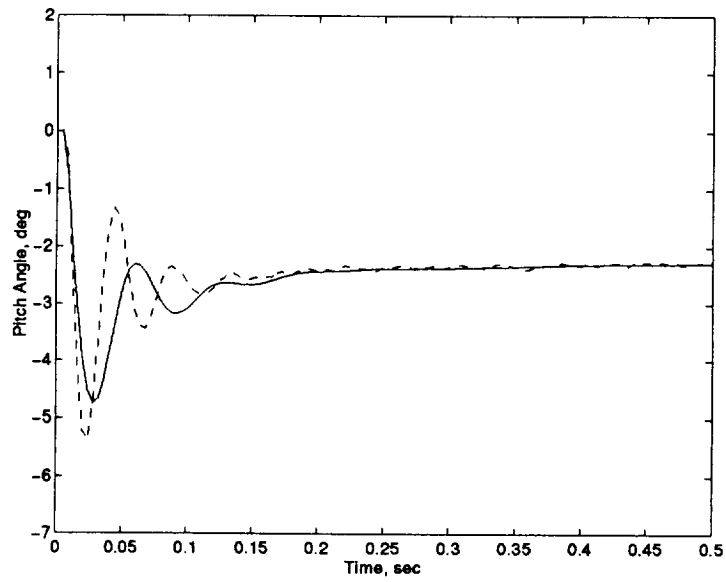


Figure 5: Analytic model simulation (solid) and experiment (dashed), pitch step response

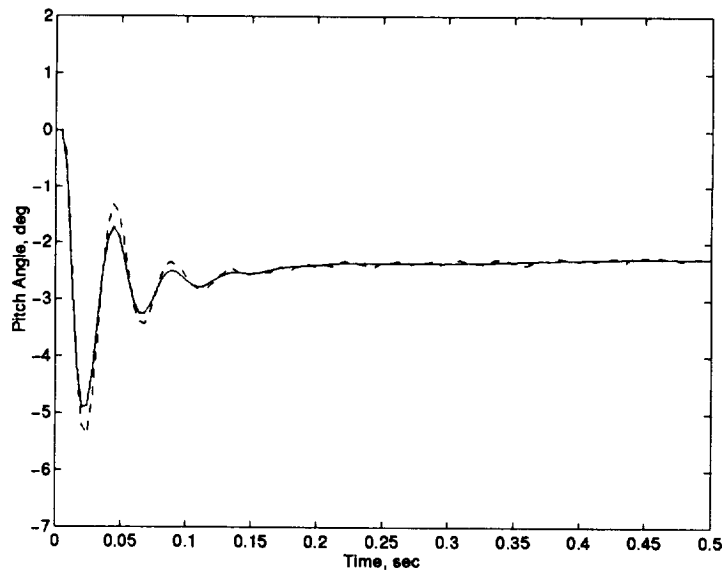


Figure 6: Identified model simulation (solid) and experiment (dashed), pitch step response

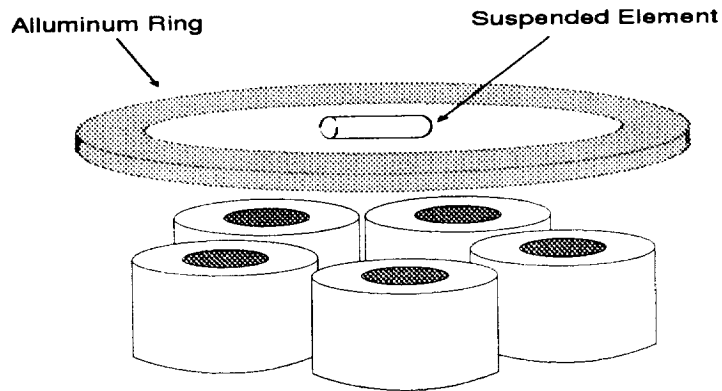


Figure 7: Perturbed LAMSTF system with aluminum ring to provide source of eddy-currents

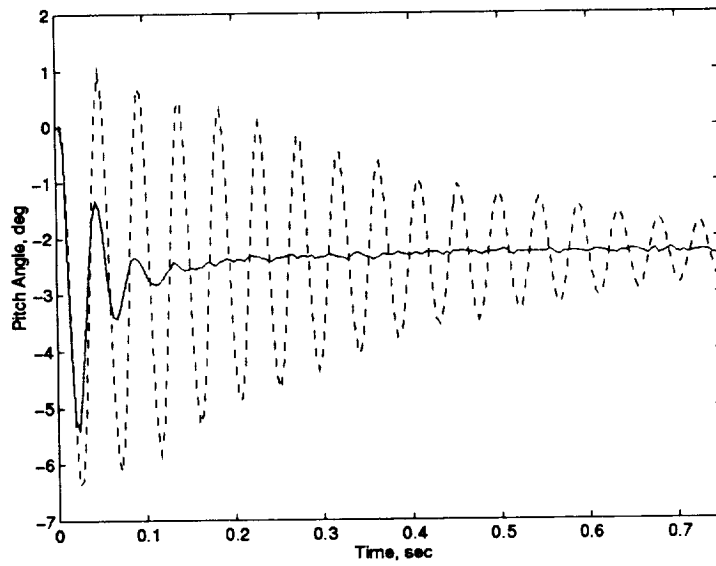


Figure 8: Nominal experiment (solid) and perturbed experiment (dashed), pitch step response

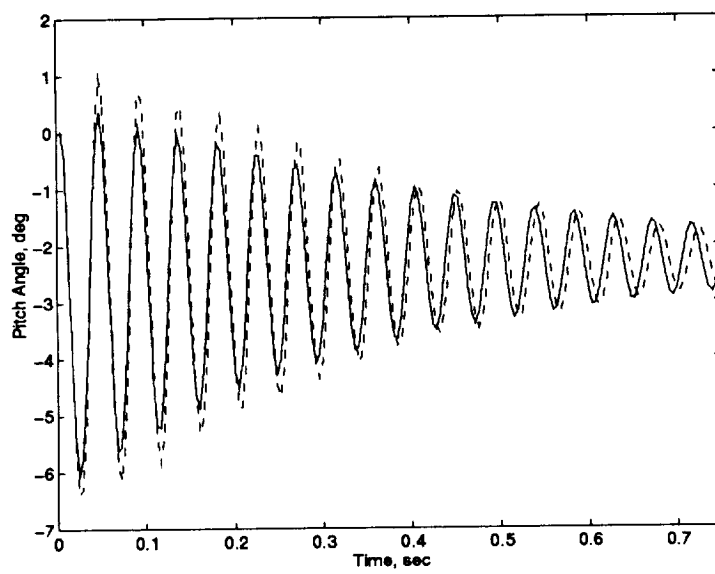


Figure 9: Identified model simulation (solid) and perturbed experiment (dashed), pitch step response

